Chemical Science

EDGE ARTICLE

View Article Online
View Journal | View Issue

Cite this: *Chem. Sci.*, 2019, **10**, 4220

All publication charges for this article have been paid for by the Royal Society of Chemistry

Dinuclear Hg^{II} tetracarbene complex-triggered aggregation-induced emission for rapid and selective sensing of Hg^{2+} and organomercury species†‡

Bin Yuan,[a] Dong-Xia Wang,[b] Li-Na Zhu,[a] Yan-Long Lan,[a] Meng Cheng,[a] Li-Ming Zhang,[a] Jun-Qing Chu,[a] Xiao-Zeng Li*[a] and De-Ming Kong*[b]

Rapid, reliable and highly selective detection of mercury species, including Hg^{2+} ions and organomercury, is of significant importance for environmental protection and human health. Herein, a new fluorescent dye 1,1,2,2-tetrakis[4-(3-methyl-1*H*-benzimidazol-1-yl)phenyl ethylene tetraiodide (**Tmbipe**) with aggregation-induced emission (AIE) potential was prepared and characterized. The presence of four positively charged methylated benzimidazole groups endows **Tmbipe** with excellent water solubility and almost undetectable background fluorescence. However, it can coordinate with two Hg^{2+} ions or two organomercury molecules (*e.g.* methylmercury and phenylmercury) to form a planar dinuclear Hg^{II} tetracarbene complex, which can then self-aggregate to turn on AIE fluorescence. Such a fluorescence turn-on process can be completed in 3 min. In addition, synergic rigidification of the tetraphenylethylene-bridged **Tmbipe** molecule by mercury-mediated chelate ring formation and subsequent aggregation results in obviously higher fluorescence enhancement than that given by the single aggregation-induced one. Low background, high fluorescence enhancement and rapid response time make **Tmbipe** a good fluorescent probe for reliable, sensitive and highly selective quantitation of both inorganic and organic mercury species. This probe was also demonstrated to work well for identification of mercury species accumulation in living cells.

Received 21st December 2018
Accepted 5th March 2019

DOI: 10.1039/c8sc05714a

rsc.li/chemical-science

Introduction

Mercury is generally acknowledged as one of the most toxic and dangerous metal ions because of its well-characterized toxicological features.[1] Even at low concentrations, mercury is highly toxic. Mercury can spread through air, water and oil. And what's worse, it can accumulate through the food chain and atmospheric circulation.[2] Exposure to mercury can cause serious environmental and health threats. It has been found that mercury damages the kidneys, especially renal proximal tubular epithelial cells. Mercury can also cause immune dysfunction, nephrotic syndrome and glomerulonephritis. In addition, it can harm the brain, nerves and endocrine system.[3]

Great efforts have been made in the sensitive and selective detection of mercury. High performance liquid chromatography (HPLC),[4] gas chromatography (GC),[5] atomic absorption spectroscopy (AAS),[6] capillary electrophoresis,[7] inductively coupled plasma mass spectrometry (ICP-MS),[8] neutron activation analysis,[9] anodic stripping voltammetry,[10] and X-ray fluorescence spectrophotometry[11] are the commonly used techniques for mercury detection. The main limitations of these methods lie in valuable, complex instruments, long data-acquisition time, and the requirement of professionally trained personnel. In the past decades, a great number of fluorescent probes and elegantly designed DNA-based biosensors have been reported for mercury detection.[12] Though highly sensitive and selective, most of these methods only give response to Hg^{2+} ions and cannot work for other mercury species.[12a,b]

In fact, when mercury is released into the environment during various natural events or due to human activities, inorganic mercury can be converted into organic forms (*e.g.* methylmercury, $MeHg^{+}$) by anaerobic microorganisms.[13] In addition, organomercury is much more poisonous than its inorganic form.[14] The reason is that the fat-soluble property enables organomercury compounds to easily pass through biofilms and act as deadly neurotoxins for many eukaryotes including fish,

[a]*Department of Chemistry, School of Science, Tianjin University, Collaborative Innovation Center of Chemical Science and Engineering, Tianjin, 300072, People's Republic of China. E-mail: linazhu@tju.edu.cn; lixiaozeng321@tju.edu.cn*

[b]*Tianjin Key Laboratory of Biosensing and Molecular Recognition, Nankai University, Tianjin, 300071, People's Republic of China. E-mail: kongdem@nankai.edu.cn*

† This work is dedicated to Professor Dai-Zheng Liao on the occasion of his 80th birthday.

‡ Electronic supplementary information (ESI) available. See DOI: 10.1039/c8sc05714a

animals, and humans,[15] leading to prenatal brain injury, cognitive and motor impairment, visual acuity, hearing loss, *etc.*[16] It has been reported that more than 80% mercury in human blood exists in the methyl form.[17] Therefore, the development of a cost- and labour-effective sensing platform showing highly sensitive and selective response to both Hg^{2+} and organomercury is still urgently required.

As a newly discovered photophysical phenomenon, aggregation-induced emission (AIE) has attracted more and more attention in recent years, and has great promising potential for sensing and bioimaging applications.[18] In this work, we prepared a new water soluble AIE dye (1,1,2,2-tetrakis [4-(3-methyl-1*H*-benzimidazol-1-yl)phenyl]ethylene tetraiodide, **Tmbipe**, Scheme 1) that could rapidly coordinate with Hg(II) species to form a dinuclear Hg^{II} tetracarbene complex, and thus reported a novel sensing strategy for the sensitive and selective detection of both Hg^{2+} ions and organic mercury (including methylmercury and phenylmercury ($PhHg^+$)). Different from traditional AIE-active mechanisms, the fluorescence response of **Tmbipe** to Hg(II) species relies on two successive processes: mercury-mediated chelate ring formation and subsequent aggregation. Synergic rigidification of **Tmbipe** molecules by these two processes could give significant fluorescence enhancement and thus improved Hg^{2+} detection sensitivity. This probe was also demonstrated to work well for imaging detection of mercury species in living cells.

Results and discussion

Tmbipe preparation and its interaction with Hg(II) species

To achieve the sensitive detection of both Hg^{2+} ions and organomercury, a water-soluble AIE dye **Tmbipe** was designed and prepared following the synthetic route shown in Scheme S1.‡ Briefly, the precursor 1,1,2,2-tetrakis[4-(1*H*-benzimidazol-1-yl) phenyl]ethylene (**Tbipe**) was synthesized according to the reported method (Fig. S1‡).[19] That is, the symmetric McMurry coupling reaction was used to prepare **Tbipe** in high yield. Then simple Hofmann alkylation between **Tbipe** and methyl iodide was carried out in dichloromethane to obtain the target probe **Tmbipe**. The details of the synthesis and characterization of **Tmbipe** are available in the ESI (Fig. S2 and S3‡). The results of both ^{1}H-nuclear magnetic resonance (^{1}H-NMR) and high resolution mass spectrometry (HRMS) characterization confirm the successful preparation of high purity **Tbipe** and **Tmbipe** with a chemical structure as shown in Scheme 1. Due to the presence of four positively charged methylated benzimidazole groups, **Tmbipe** shows excellent water solubility.

The tetraphenylethylene skeleton endows **Tmbipe** with typical AIE-based fluorescence features.[20] Thus, the fluorescence property of **Tmbipe** was investigated. Both the C–C bonds between phenyl rings and C=C bonds and the C–N bonds between phenyl rings and benzimidazoles show high rotation tendencies (Scheme 1), which not only reduces the molecular planarity but also increases the possibility of radiationless relaxation, thus conferring **Tmbipe** with negligible fluorescence emission in aqueous solution. However, we were pleased to find that addition of Hg^{2+} and organomercury (*e.g.* $MeHg^+$ and $PhHg^+$) could result in significant enhancement of the fluorescence emission (Fig. 1), thus suggesting that **Tmbipe** might be used as a fluorescent probe for convenient detection of both Hg^{2+} and organomercury.

To understand why Hg^{2+} and organomercury can turn on the fluorescence of **Tmbipe**, the interactions between **Tmbipe** and Hg^{2+} (and organomercury) were investigated. First of all, Job's plot analysis was used to determine the binding stoichiometry between them. The results showed that **Tmbipe** bound to Hg^{2+}, $MeHg^+$ and $PhHg^+$ with the same stoichiometry of 1 : 2 (Fig. S4‡), indicating that one **Tmbipe** molecule can bind with two molecules of Hg(II) species. The above results suggested that **Tmbipe** might bind to Hg^{2+} ions and organomercury in a similar manner.

Then, UV-vis and infrared (IR) absorption spectroscopies were used to further elucidate the binding interactions between **Tmbipe** and mercury species. Since the Hg^{2+} ion itself gives much simpler UV-vis and IR absorption signals than organomercury species, the IR and UV-vis spectra of the **Tmbipe**/Hg^{2+} mixture were recorded and compared with that of **Tmbipe** (Fig. 2). The UV-vis spectrum of **Tmbipe** showed an absorption peak at 265 nm. With the addition of increasing concentrations

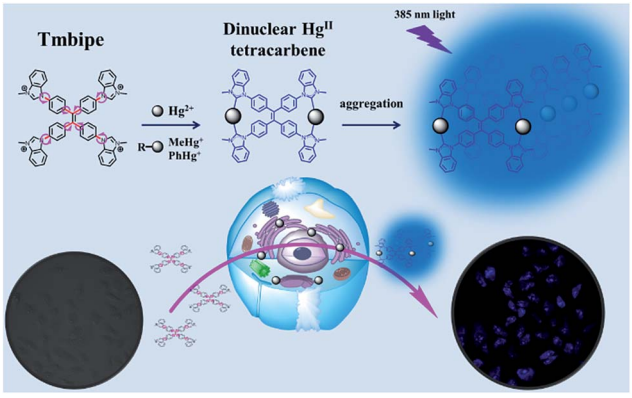

Scheme 1 Structure of **Tmbipe** and its use in the detection of inorganic and organic mercury.

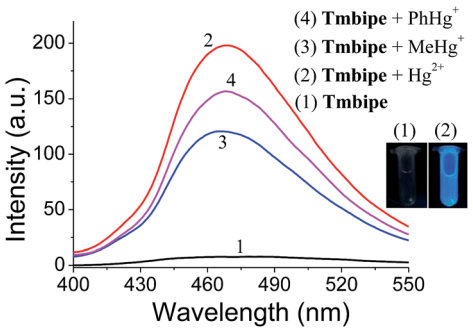

Fig. 1 Fluorescence spectra of **Tmbipe** in the absence and presence of Hg^{2+}, $MeHg^+$ or $PhHg^+$. [**Tmbipe**] = 10 μM; [Hg^{2+}] = [$MeHg^+$] = [$PhHg^+$] = 20 μM. The inset shows the aqueous solution photograph of **Tmbipe** in the absence and presence of Hg^{2+} under UV light irradiation.

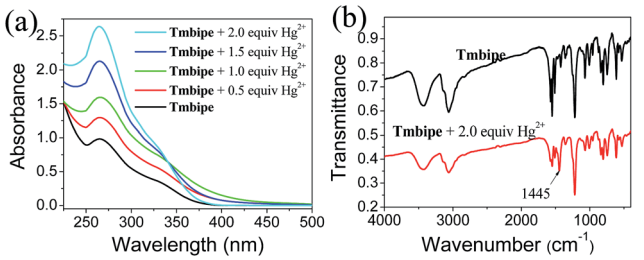

Fig. 2 UV-vis (a) and IR (b) spectra of **Tmbipe** in the absence or presence of Hg^{2+}.

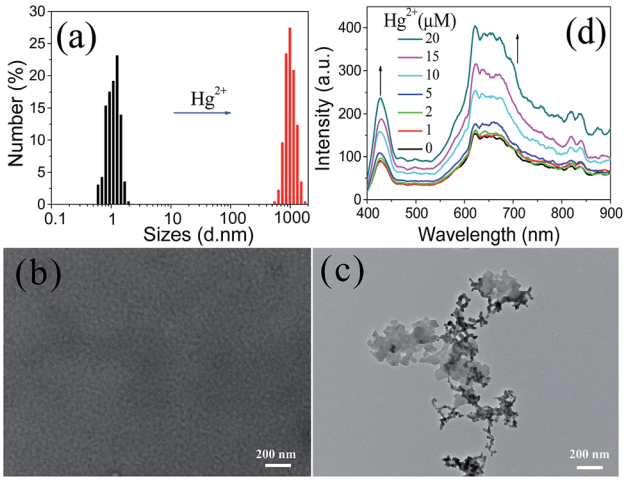

Fig. 3 (a) DLS, (b and c) TEM and (d) RLS characterization of **Tmbipe** in the absence and presence of Hg^{2+}. In (a) and (c), 2.0 equiv. of Hg^{2+} was added.

of Hg^{2+}, the peak intensity continuously increased, which might be attributed to the coordination of mercury ions with **Tmbipe**.[21] Interestingly, when the concentration ratio of Hg^{2+} to **Tmbipe** exceeded 1.0, an isosbestic point was observed at 340 nm, indicating that two **Tmbipe**/Hg^{2+} complexes existed in the mixture: one might be the complex with a stoichiometric ratio of 1 : 1, and the other might be the one with a stoichiometric ratio of 1 : 2. That is to say, in the low Hg^{2+} concentration range, one **Tmbipe** molecule preferentially binds with one Hg^{2+} ion to form a 1 : 1 complex. With the further addition of Hg^{2+} ions, the 1 : 1 complex will bind with a second Hg^{2+} ion to form the 1 : 2 complex. The IR spectrum of the **Tmbipe**/Hg^{2+} mixture clearly shows a new band centered at 1445 cm^{-1} compared to that of free **Tmbipe**, suggesting the existence of C–Hg bonds in the complex formed by Hg^{2+} and **Tmbipe**.[18b] Therefore, it can be speculated that one mercury atom simultaneously coordinates with two benzimidazole groups to form a dinuclear Hg^{II} tetracarbene complex **Hg_2Tmbipe**, in which two 15-membered macrocycles are contained (Scheme 1).

Formation of the closed macrocycles could "lock" the free rotation of both C–N and C–C bonds in **Tmbipe**, resulting in a great increase of molecular planarity. Such a rigidification of the tetraphenylethylene-bridged **Tmbipe** molecule suppresses the radiationless deactivation pathways. As a result, the fluorescence of **Tmbipe** is turned on. A similar complexation reaction has recently been used by Sinha *et al.* to prepare dinuclear Ag^{I} and Au^{I} tetracarbene complexes using two tetraphenylethylene-bridged tetraimidazolium salts as precursors.[21a] Different from the fact that a relatively long reaction time (2 days) and high temperature (60 °C) are required for Ag^{I} and Au^{I} tetracarbene complex formation, our **Hg_2Tmbipe** can be readily formed at ambient temperature, which is reflected by the fact that a stable and strong fluorescence signal output can be obtained within 3 min after Hg^{2+} addition (Fig. S5‡). Such a rapid signal response makes **Tmbipe** an excellent candidate for fluorescence sensing of mercury species.

Since **Tmbipe** shares common structural characteristics of AIE dyes, we want to determine if the mercury species-induced fluorescence enhancement is related with aggregation of **Tmbipe** or not. To answer this question, several techniques, including transmission electron microscopy (TEM), dynamic light scattering (DLS) and resonance light scattering (RLS), were used to characterize the morphology and size changes of **Tmbipe** before and after Hg^{2+} addition. DLS results (Fig. 3a) showed that free **Tmbipe** had an average size about 1.3 nm, indicating that it was monodisperse in solution. Addition of 2.0 equiv. of Hg^{2+} resulted in a sharp increase of the hydrodynamic size to around 1000 nm, suggesting the formation of large aggregates. The results of TEM characterization also demonstrated the Hg^{2+}-induced aggregation of **Tmbipe**. As shown in Fig. 3b and c, almost no observable nanoparticles are shown in the TEM image of free **Tmbipe**. After addition of 2.0 equiv. of Hg^{2+}, however, big clumps are clearly observed, thus giving direct evidence for **Tmbipe** aggregation in the presence of Hg^{2+}. RLS is also an effective technique for studying the aggregation behavior of dyes. As shown in Fig. 3d, the RLS intensities of **Tmbipe** continuously increased with Hg^{2+} concentration, further demonstrating the size increase caused by Hg^{2+}-induced aggregation. Collectively, when **Tmbipe** is mixed with Hg^{2+} ions, it will rapidly coordinate with two Hg^{2+} ions to form a highly planar dinuclear Hg^{II} tetracarbene complex, **Hg_2Tmbipe**. The increase in molecular planarity can then promote the self-aggregation of **Hg_2Tmbipe** *via* hydrophobic and π–π interactions. The formation of aggregates might further restrict the skeletal vibration of **Tmbipe** molecules, thus giving strong AIE fluorescence.

Selection of solvent for sensitive mercury species quantitation

Tmbipe is water soluble. This makes mercury species detection in pure aqueous media possible. However, we noticed that a very weak background fluorescence could also be observed without mercury species addition in pure aqueous solution (Fig. 4). To give a high signal-to-noise ratio in mercury species detection, it is best to decrease the background to a negligible level. Therefore, a suitable solvent system was screened. Fig. 4 shows the fluorescence change of **Tmbipe** in water/tetrahydrofuran (THF)-mixed solvents. In 100% aqueous solution, **Tmbipe** showed a very weak fluorescence, which might be attributed to the slight self-aggregation due to the hydrophobic and π–π interactions of the tetraphenylethene skeleton of **Tmbipe**. This self-aggregation was easily destroyed when

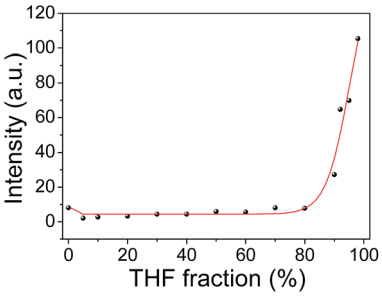

Fig. 4 Fluorescence intensity of **Tmbipe** at 468 nm in different solvents.

a small amount of THF (*e.g.* 5%) was added, accompanied by the decrease of the fluorescence to a negligible level. The low background was maintained when the fraction of THF was increased to 80%. After that, the fluorescence significantly increased with the THF volume fraction, which can be rationally interpreted by the emergence of the AIE signal due to the aggregation of water-soluble **Tmbipe** in organic solvent. Therefore, a mixed solvent (5% THF–water) was used as the working solvent system for subsequent ultralow background detection of mercury species.

It should be noted that Hg^{2+}-induced fluorescence signal enhancement (Fig. 1 and 5) was much higher than that induced by solvent. This can be reasonably interpreted by their different working mechanisms. That is, in our Hg^{2+}-induced aggregation system, the radiationless deactivation of **Tmbipe** can be overcome in two ways: formation of a planar dinuclear Hg^{II} tetracarbene complex with two chelate rings and subsequent aggregation of the tetracarbene complex. Such a synergic rigidification of tetraphenylethylene-bridged **Tmbipe** molecules can give significantly enhanced fluorescence. Such a highly efficient fluorescence enhancement mechanism is beneficial for the sensitive detection of Hg^{2+} ions. In a solvent-induced aggregation system, however, only aggregation but no chelate ring formation-induced probe molecule rigidification is used to turn on fluorescence. The effects of pH on the fluorescence response of **Tmbipe** to Hg^{2+} and organomercury species were also investigated. The results (Fig. S6‡) showed that pH had little effect on the fluorescence signals of the sensing systems, indicating that **Tmbipe** can be used for the detection of Hg^{2+} and organomercury species in a broad pH range.

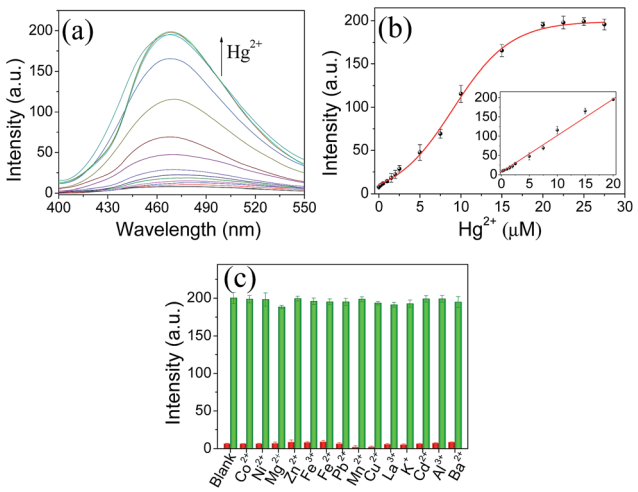

Fig. 5 Quantitation of Hg^{2+}. (a) Fluorescence spectra of the sensing systems containing different concentrations of Hg^{2+}. (b) Hg^{2+} concentration-dependent changes in fluorescence intensity at 468 nm. The inset shows the linear relationship between the fluorescence intensity and Hg^{2+} concentration in the range of 200 nM–20 μM. (c) Selectivity of the Hg^{2+}-sensing system. The red bars represent the fluorescence signals of the sensing systems in the presence of 100 μM other metal ions. The green bars represent the fluorescence signals of the sensing systems containing 20 μM Hg^{2+} and 100 μM other metal ions.

Sensitivity and selectivity of Hg^{2+} quantitation

Having demonstrated the feasibility of Hg^{2+} detection using **Tmbipe** as the AIE probe, the detection sensitivity was evaluated by recording the fluorescence response of the proposed sensing platform towards different concentrations of Hg^{2+}. As shown in Fig. 5, Hg^{2+} concentration-dependent fluorescence signal increase was given by the sensing system, and a linear relationship ($I = 6.44 + 9.50C$ (μM), $R^2 = 0.9962$) between the fluorescence intensity and Hg^{2+} concentration was observed in the range of 200 nM–20 μM. Based on the rule of $3\sigma/S$, the detection limit was calculated to be 63 nM.

The prepared Hg^{2+} probe exhibits good detection selectivity, which was demonstrated by testing the response of **Tmbipe** to other metal ions with 5 times the concentration of Hg^{2+} (Fig. 5c). None of these competitive metal ions, including Co^{2+}, Ni^{2+}, Mg^{2+}, Zn^{2+}, Fe^{3+}, Fe^{2+}, Pb^{2+}, Mn^{2+}, Cu^{2+}, La^{3+}, K^{+}, Cd^{2+}, Al^{3+} and Ba^{2+}, could give an observable increase of fluorescence intensity, demonstrating the high selectivity of the probe for Hg^{2+} quantitation. More interestingly, the selectivity of **Tmbipe** was so high that it enabled selective Hg^{2+} detection even in the mixture of Hg^{2+} and other challenging metal ions. That is, when Hg^{2+} and another metal ion (5 times the Hg^{2+} concentration) were both added to the sensing system, the fluorescence signal increased to a level similar to that when Hg^{2+} alone was added, thus indicating that Hg^{2+} detection would not be interfered with by the presence of other metal ions. Such a high selectivity might be attributed to the formation of dinuclear Hg^{II} tetracarbene complexes, which requires the coordination of Hg^{2+} with carbon atoms in benzimidazole groups. Compared to other metal ions, Hg^{2+} has a much higher tendency to coordinate with carbon atoms, which can be demonstrated by the high conversion rate of Hg^{2+} to $MeHg^{+}$ in the natural environment and extraordinary stability of $MeHg^{+}$ in a hot sulfuric acid solution.[22]

Quantitation of organomercury compounds

Considering that organomercury is much more poisonous than Hg^{2+} due to its good lipid solubility, the sensitive and reliable detection of organomercury is more striking. Therefore, the feasibility of organomercury quantitation using the proposed sensing system was investigated by recording the changes in fluorescence intensity of **Tmbipe** (10 μM) as

a function of organomercury concentration (Fig. 6). First, the applicability for $MeHg^+$ detection was tested. Encouragingly, **Tmbipe** could also give a rapid fluorescence response to $MeHg^+$, and about 16-fold fluorescence intensity increase was observed after addition of 2.0 equiv. of $MeHg^+$. A good relationship ($I = 8.57 + 6.31C$ (μM), $R^2 = 0.9902$) was observed between fluorescence intensity and $MeHg^+$ concentration in the range of 200 nM–20 μM. The detection limit was calculated to be 94 nM. To date, only a few fluorescent probes that can work for both Hg^{2+} and $MeHg^+$ have been reported.[18b,23] Compared to these probes, our **Tmbipe** shows comparable or better detection sensitivity (Table S1‡). Besides $MeHg^+$, $PhHg^+$, another organomercury species could also be easily detected by **Tmbipe** in the same way. The linear detection range was 200 nM–20 μM ($I = 7.68 + 7.62C$ (μM), $R^2 = 0.9961$) and the detection limit was 78 nM. These results, combined with those of Job plot analysis, suggested that both Hg^{2+} ions and organomercury can coordinate with **Tmbipe** to form dinuclear Hg^{II} tetracarbene complexes and AIE-active aggregates, thus making the simultaneous detection of inorganic and organic mercury species possible.

Fluorescence imaging in living cells

Having demonstrated the ability of **Tmbipe** to quantitatively detect Hg^{2+} ions and organomercury, its bioimaging application in detecting Hg(II) species in living cells was then explored. To achieve this, human cervical carcinoma HeLa cells were divided into three groups: one group was incubated with 10 μM **Tmbipe** probe for 30 min and the other two groups were treated with 10 μM or 20 μM Hg^{2+} for 1 h, respectively, followed by incubation with 10 μM **Tmbipe** for 30 min after removing non-accumulated Hg^{2+}. As shown in Fig. 7, no evidence of fluorescence appeared

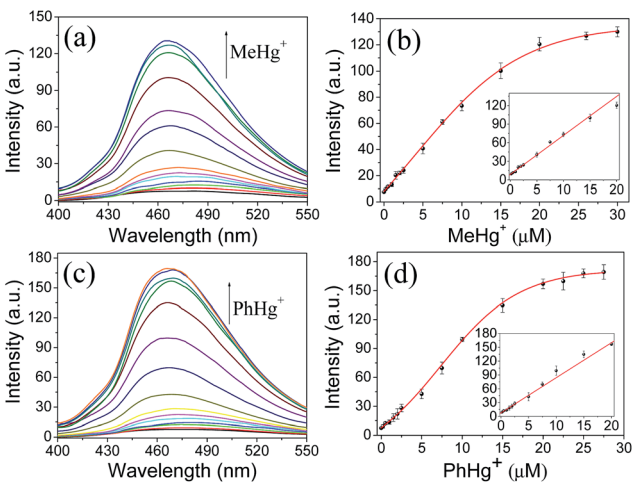

Fig. 6 Quantitation of (a and b) $MeHg^+$ or (c and d) $PhHg^+$ using the **Tmbipe** probe. (a and c) Fluorescence spectra of the sensing systems containing different concentrations of (a) $MeHg^+$ or (c) $PhHg^+$. (b and d) $MeHg^+$ or $PhHg^+$ concentration-dependent changes in fluorescence intensity at 468 nm. The insets show the linear relationship between the fluorescence intensity and $MeHg^+$ or $PhHg^+$ concentration in the range of 200 nM–20 μM.

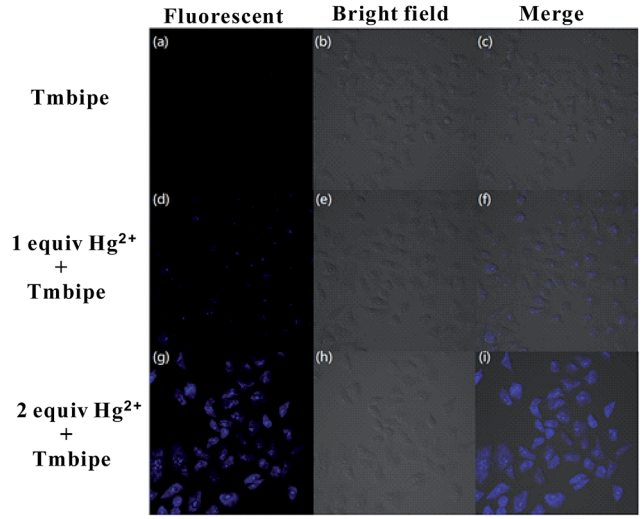

Fig. 7 Detection of Hg(II) species in HeLa cells.

in the HeLa cells without Hg^{2+} treatment, indicating that **Tmbipe** remained in a dispersed state in living cells containing no Hg(II) species. In contrast, blue fluorescence was observed from the cells contaminated with 1.0 equiv. of Hg^{2+}, suggesting that probe molecules can efficiently pass through cell membranes and coordinate with intracellular Hg(II) species, giving an active fluorescence signal. When the Hg^{2+} concentration was increased to 2.0 equivalents, the fluorescence intensity was significantly enhanced, demonstrating that the observed fluorescence intensity is concentration-dependent. Similar results were observed for Hg(II)-imaging in HL7704 human adult hepatocyte cells and MCF-7 human breast cancer cells (Fig. S7‡). These results suggest that the prepared **Tmbipe** probe is able to detect the accumulation of mercury species in living cells.

Conclusions

In summary, a new water-soluble AIE-based fluorescent probe, **Tmbipe**, which contains a tetraphenylethylene-bridged skeleton and four positively charged benzimidazole groups, was designed, synthesized and well characterized. This probe could coordinate with both Hg^{2+} and organomercury to form planar dinuclear Hg^{II} tetracarbene complexes, which would self-aggregate to give active AIE fluorescence. Synergic rigidification of the tetraphenylethylene-bridged **Tmbipe** molecule by mercury-mediated chelate ring formation and subsequent aggregation could result in higher fluorescence enhancement than that given by single aggregation-induced AIE activation. The fluorescence response of **Tmbipe** to Hg(II) species was so rapid that it could reach a maximum in 3 min. The unique dinuclear Hg^{II} tetracarbene formation-based working mechanism endows **Tmbipe** with highly specific response towards Hg^{2+} and organomercury species. These attractive characteristics endow **Tmbipe** with the ability to sensitively and selectively detect both Hg^{2+} ion and organomercury species. This probe was also demonstrated to work well for the detection of mercury species accumulation in living cells.

Experimental

Materials and reagents

Methylmercury, phenylmercury, iodomethane, 1*H*-benzimidazole and 4,4′-difluorobenzophenone were obtained from Sigma. $TiCl_4$, tetrahydrofuran (THF), copper power, dimethyl sulfoxide (DMSO), zinc powder, ethyl acetate, diethyl ether and other metal salts ($Hg(Ac)_2$, $Co(Ac)_2$, $Ni(NO_3)_2$, $Mg(NO_3)_2$, $Zn(Ac)_2$, $Fe(NO_3)_3$, $Fe(NO_3)_2$, $Pb(NO_3)_2$, $Mn(Ac)_2$, $Cu(NO_3)_2$, $La(NO_3)_3$, KAc, $Cd(NO_3)_2$, $Al(NO_3)_3$ and $Ba(NO_3)_2$) were obtained from Jiangtian Co. Ltd. (Tianjin, China). Deionized and sterilized water (resistance > 18 MΩ cm^{-1}) was used in all the experiments. All chemical reagents were of analytical grade and used without further purification.

Instruments and measurements

The ^{1}H-nuclear magnetic resonance (^{1}H-NMR) spectra were recorded in DMSO-d_6 on a Bruker Spectrospin Avance 400 MHz NMR spectrophotometer. Chemical shifts are given in ppm downfield from tetramethylsilane. Infrared (IR) spectra were measured on a Perkin Elmer Spectrum One spectrophotometer. UV-vis absorption spectra were recorded on a Cary 60 UV-vis spectrophotometer (Agilent Technologies). High resolution mass spectrometry (HRMS) was carried out using an Agilent 6520 Q-TOF LC/MS mass spectrometer. Elemental analysis was performed on a Perkin-Elmer 240 elemental analyzer. Fluorescence spectra and resonance light scattering (RLS) spectra were measured at room temperature using a SHIMADZU RF-5301PC spectrofluorimeter. The transmission electron micrograph (TEM) images were recorded on a German Leica TCS-SP8 transmission electron microscope. A Malvern Zetasizer Nano ZS90 particle size analyzer was used for dynamic light scattering (DLS) studies.

Synthesis and characterization of Tmbipe

The synthetic route to **Tmbipe** is shown in Scheme S1.‡ The precursor **Tbipe** was synthesized according to the reported method.[19] Its ^{1}H-NMR spectrum is given in Fig. S1.‡ Then, the compound **Tbipe** (0.500 g, 0.630 mmol) and an excess of iodomethane (0.716 g, 5.040 mmol) were dissolved in 10 mL of dry dichloromethane. The obtained reaction mixture was heated to reflux for 48 h. During this period, a pale yellow precipitate was generated. After cooling of the reaction mixture to ambient temperature, the precipitate was isolated by filtration, washed with diethyl ether and then dried *in vacuo* to give a pale yellow solid. ^{1}H-NMR (400 MHz, DMSO-d_6), δ = 10.18 (s, 4H), 8.16 (d, 4H), 7.79–7.83 (m, 16H), 7.70–7.72 (d, 4H), 7.61–7.63 (d, 8H), 4.18 ppm (s, 12H); HRMS (ESI, positive ions): m/z = 214.0998 (calcd for $Tmbipe^{4+}$ = 214.2682). Elemental analysis calcd (%) for $C_{58}H_{48}N_8I_4$: C, 51.05; H, 3.55; N, 8.21; found: C, 51.15; H, 3.42; N, 8.09.

Detection of Hg^{2+} and organomercury

A stock solution of **Tmbipe** (1 mM) was prepared in deionized water. The mixture of 10 μM **Tmbipe** and different concentrations of Hg^{2+}, methylmercury or phenylmercury was prepared in a mixed solvent (THF : H_2O = 5 : 95). After incubation at ambient temperature for 3 min, the fluorescence spectrum in the range of 400–550 nm was recorded under the excitation of 385 nm (excitation slit = emission slit = 5 nm), and the fluorescence intensity at 468 nm was used for mercury species quantitation.

Detection of Hg(II) species in living cells

HeLa cells and MCF-7 cells were cultured in Dulbecco's modified Eagle's medium (DMEM) supplemented with 10% fetal bovine serum (FBS). HL 7702 cells were cultured in RPMI 1640 medium supplemented with 10% FBS. Cells in the exponential phase of growth were seeded into 24 well plates and then incubated with 10 μM or 20 μM Hg^{2+} for 1 h at 37 °C. After being washed three times with PBS, the cells were incubated with 10 μM **Tmbipe** for another 30 min. Then, the cells were washed three times with PBS buffer. Fluorescence imaging of living cells was performed on an Olympus IX-81 microscope.

Conflicts of interest

There are no conflicts to declare.

Acknowledgements

This work was supported by the National Natural Science Foundation of China (no. 21371130 and 21728801), the Natural Science Foundation of Tianjin (no. 15JCYBJC48300 and 16JCYBJC19900), and the Innovation Fund of Tianjin University.

Notes and references

1 K. H. Kim, E. Kabir and S. A. Jahan, *J. Hazard. Mater.*, 2016, **306**, 376.
2 C. O. R. Okpala, G. Sardo, S. Vitale, G. Bono and A. Arukwe, *Crit. Rev. Food Sci. Nutr.*, 2018, **58**, 1986.
3 J. D. Park and W. Zheng, *J. Prev. Med. Public Health*, 2012, **45**, 344.
4 J. Delafiori, G. Ring and A. Furey, *Talanta*, 2016, **153**, 306.
5 G. A. Zachariadis, *J. Chromatogr. A*, 2013, **1296**, 47.
6 H. Bagheri and M. Naderi, *J. Hazard. Mater.*, 2009, **165**, 353.
7 X. P. Yan, X. B. Yin, D. Q. Jiang and X. W. He, *Anal. Chem.*, 2003, **75**, 1726.
8 C. Y. Peng, M. He, B. B. Chen, L. J. Huang and B. Hu, *Analyst*, 2017, **142**, 4570.
9 P. Movalli, P. Bode, R. Dekker, L. Fornasari, S. Van der Mije and R. Yosef, *Environ. Sci. Pollut. Res.*, 2017, **24**, 25986.
10 E. S. Almeida, E. M. Richter and R. A. A. Munoz, *Anal. Chim. Acta*, 2014, **837**, 38.
11 G. Elias, E. Margui, S. Diez and C. Fontas, *Anal. Chem.*, 2018, **90**, 4756.
12 (*a*) H. N. Kim, W. X. Ren, J. S. Kim and J. Yoon, *Chem. Soc. Rev.*, 2012, **41**, 3210; (*b*) E. M. Nolan and S. J. Lippard, *Chem. Rev.*, 2008, **108**, 3443; (*c*) J. Chan, S. C. Dodani and

C. J. Chang, *Nat. Chem.*, 2012, **4**, 973; (*d*) W. Cai, S. B. Xie, J. Zhang, D. Y. Tang and Y. Tang, *Biosens. Bioelectron.*, 2017, **98**, 466; (*e*) H. Xie, Q. Wang, Y. Q. Chai, Y. L. Yuan and R. Yuan, *Biosens. Bioelectron.*, 2016, **86**, 630; (*f*) X. L. Liang, L. Wang, D. Wang, L. W. Zeng and Z. Y. Fang, *Chem. Commun.*, 2016, **52**, 2192; (*g*) P. Zheng, M. Li, R. Jurevic, S. K. Cushing, Y. X. Liu and N. Q. Wu, *Nanoscale*, 2015, **7**, 11005; (*h*) B. Tang, B. Y. Ding, K. H. Xu and L. L. Tong, *Chem.–Eur. J.*, 2009, **15**, 3147; (*i*) Y. C. Chen, W. J. Zhang, Y. J. Cai, R. T. K. Kwok, Y. B. Hu, J. W. Y. Lam, X. G. Gu, Z. K. He, Z. Zhao, X. Y. Zheng, B. Chen, C. Gui and B. Z. Tang, *Chem. Sci.*, 2017, **8**, 2047; (*j*) N. Zhao, J. W. Y. Lam, H. H. Y. Sung, H. M. Su, I. D. Williams, K. S. Wong and B. Z. Tang, *Chem.–Eur. J.*, 2014, **20**, 133; (*k*) X. J. Liu, C. Qi, T. Bing, X. H. Cheng and D. H. Shangguan, *Anal. Chem.*, 2009, **81**, 3699; (*l*) S. J. Wang, X. Li, J. Q. Xie, B. Y. Jiang, R. Yuan and Y. Xiang, *Sens. Actuators, B*, 2018, **259**, 730; (*m*) W. H. Wang, T. S. Kang, P. W. H. Chan, J. J. Lu, X. P. Chen, C. H. Leung and D. L. Ma, *Sci. Technol. Adv. Mater.*, 2015, **16**, 065004; (*n*) D. S. H. Chan, H. M. Lee, C. M. Che, C. H. Leung and D. L. Ma, *Chem. Commun.*, 2009, **48**, 7479; (*o*) X. J. Xue, F. Wang and X. G. Liu, *J. Am. Chem. Soc.*, 2008, **130**, 3244; (*p*) S.-M. Jia, X.-F. Liu, P. Li, D.-M. Kong and H.-X. Shen, *Biosens. Bioelectron.*, 2011, **27**, 148; (*q*) D.-M. Kong, N. Wang, X.-X. Guo and H.-X. Shen, *Analyst*, 2010, **135**, 545; (*r*) Q. Zhang, Y. Cai, H. Li, D.-M. Kong and H.-X. Shen, *Biosens. Bioelectron.*, 2012, **38**, 331; (*s*) Q. Duan, X. Lv, C. Liu, Z. Geng, F. Zhang, W. Sheng, Z. Wang, P. Jia, Z. Li, H. Zhu and B. Zhu, *Ind. Eng. Chem. Res.*, 2019, **58**, 11; (*t*) Q. Duan, H. Zhu, C. Liu, R. Yuan, Z. Fang, Z. Wang, P. Jia, Z. Li, W. Sheng and B. Zhu, *Analyst*, 2019, **144**, 1426.

13 (*a*) K. S. Hoy, W. Feng and X. C. Le, *J. Environ. Sci.*, 2018, **68**, 218; (*b*) T. Zhang, B. Kim, C. Levard, B. C. Reinsch, G. V. Lowry, M. A. Deshusses and H. Hsu-Kim, *Environ. Sci. Technol.*, 2012, **46**, 6950; (*c*) S. M. Ullrich, T. W. Tanton and S. A. Abdrashitova, *Crit. Rev. Environ. Sci. Technol.*, 2001, **31**, 241.

14 S. Díez, *Rev. Environ. Contam. Toxicol.*, 2009, **198**, 111.

15 (*a*) F. A. Duarte, B. M. Soares, A. A. Vieira, E. R. Pereira, J. V. Maciel, S. S. Caldas and E. G. Primel, *Anal. Chem.*, 2013, **85**, 5015; (*b*) L. Yang, V. Colombini, P. Maxwell, Z. Mester and R. E. Sturgeon, *J. Chromatogr. A*, 2003, **1011**, 135.

16 K. Eto, H. Tokunaga and K. Nagashima, *Toxicol. Pathol.*, 2002, **30**, 714.

17 (*a*) J. S. Park, J. S. Lee, G. B. Kim, J. S. Cha, S. K. Shin, H. G. Kang, E. J. Hong, G. T. Chung and Y. H. Kim, *Water, Air, Soil Pollut.*, 2010, **207**, 391; (*b*) H. Akagi and A. Naganuma, *J. Health Sci.*, 2000, **46**, 323.

18 (*a*) H.-T. Feng, Y.-X. Yuan, J.-B. Xiong, Y.-S. Zheng and B.-Z. Tang, *Chem. Soc. Rev.*, 2018, **47**, 7452; (*b*) A. Chatterjee, M. Banerjee, D. G. Khandare, R. U. Gawas, S. C. Mascarenhas, A. Ganguly, R. Gupta and H. Joshi, *Anal. Chem.*, 2018, **234**, 12698; (*c*) X. Feng, C. X. Qi, H. T. Feng, Z. Zhao, H. H. Y. Sung, I. D. Williams, R. T. K. Kwok, J. W. Y. Lam, A. J. Qin and B. Z. Tang, *Chem. Sci.*, 2018, **9**, 5679; (*d*) X. Z. Yan, H. Z. Wang, C. E. Hauke, T. R. Cook, M. Wang, M. L. Saha, Z. X. Zhou, M. M. Zhang, X. P. Li, F. H. Huang and P. J. Stang, *J. Am. Chem. Soc.*, 2015, **137**, 15276.

19 S. Odabas, E. Tekin, F. Turksoy and C. Tanyeli, *J. Lumin.*, 2016, **176**, 240.

20 (*a*) J. Shi, Q. Deng, Y. Li, M. Zheng, Z. Chai, C. Wan, Z. Zheng, L. Li, F. Huang and B. Tang, *Anal. Chem.*, 2018, **90**, 13775; (*b*) S. J. Liu, Y. H. Cheng, H. K. Zhang, Z. J. Qiu, R. T. K. Kwok, J. W. Y. Lam and B. Z. Tang, *Angew. Chem., Int. Ed.*, 2018, **57**, 6274; (*c*) Q. Zhang, Y.-C. Liu, D.-M. Kong and D.-S. Guo, *Chem.–Eur. J.*, 2015, **21**, 13253; (*d*) H.-X. Jiang, M.-Y. Zhao, C.-D. Niu and D.-M. Kong, *Chem. Commun.*, 2015, **51**, 16518.

21 (*a*) N. Sinha, L. Stegemann, T. T. Y. Tan, N. L. Doltsinis, C. A. Strassert and F. E. Hahn, *Angew. Chem., Int. Ed.*, 2017, **56**, 2785; (*b*) M.-H. Yu, H.-H. Yang, A. R. Naziruddin, S. Kanne, B. H. Wang, F. C. Liu, I. J. B. Lin and G. H. Lee, *Eur. J. Inorg. Chem.*, 2016, **2016**, 4829.

22 M. Schlosser, *Organometallics in Synthesis*, 3rd edn, Wiley, New York, 2012.

23 (*a*) S.-L. Pan, K. Li, L.-L. Li, M.-Y. Li, L. Shi, Y.-H. Liu and X.-Q. Yu, *Chem. Commun.*, 2018, **54**, 4955; (*b*) M. Deng, D. Gong, S.-C. Han, X. Zhu, A. Iqbal, W. Liu, W. Qin and H. Guo, *Sens. Actuators, B*, 2017, **243**, 195; (*c*) J. Garcia-Calvo, S. Vallejos, F. C. Garcia, J. Rojo, J. M. Garcia and T. Torroba, *Chem. Commun.*, 2016, **52**, 11915; (*d*) B. Díaz de Greñu, J. García-Calvo, J. V. Cuevas, G. García-Herbosa, B. García, N. Busto, S. Ibeas, T. Torroba, B. Torroba, A. Herrera and S. Pons, *Chem. Sci.*, 2015, **6**, 3757; (*e*) L. Ding, Q. Zou and J. Su, *Sens. Actuators, B*, 2012, **168**, 185; (*f*) Q. Zou and H. Tian, *Sens. Actuators, B*, 2010, **149**, 20; (*g*) X. Chen, K.-H. Baek, Y. Kim, S.-J. Kim, I. Shin and J. Yoon, *Tetrahedron*, 2010, **66**, 4016; (*h*) Y.-K. Yang, S.-K. Ko, I. Shin and J. Tae, *Org. Biomol. Chem.*, 2009, **7**, 4590.